



IJIRCCCE

e-ISSN: 2320-9801 | p-ISSN: 2320-9798



INTERNATIONAL JOURNAL OF INNOVATIVE RESEARCH

IN COMPUTER & COMMUNICATION ENGINEERING

Volume 9, Issue 6, June 2021

ISSN INTERNATIONAL
STANDARD
SERIAL
NUMBER
INDIA

Impact Factor: 7.542



9940 572 462



6381 907 438



ijircce@gmail.com



www.ijircce.com

Lung Portion segmentation on High Resolution Computerized Tomography using: Deep Learning

Dr. P. Ammi Reddy^{*1}, Jaffar Shariff Shaik^{*2}, V.H.S.K Karthik^{*3}, Naga Dinesh Reganti⁴, Jayadeep Ravipati^{*5}

Professor, Department of ECE, Vasireddy Venkatadri Institute of Technology, Nambur, Guntur, Andhra Pradesh, India^{*1}

B.Tech Student, Department of ECE, Vasireddy Venkatadri Institute of Technology, Nambur, Guntur, Andhra Pradesh, India^{*2,3,4,5}

ABSTRACT: The aim of this work is to identify a fast, precise, automated and accurate deep learning segmentation approach, applied for the segmentation of lung portion, using a very small dataset of high-resolution computerized tomography. In this way, we aim to enhance the methodology performed by the healthcare operators in radiomics studies where the operator-independent segmentation methods must be used to correctly identify the target. Methods: we used U-Net architecture, which is already used in many bio-medical image segmentation tasks, our image dataset is composed of 42 studies of patients, of which only 32 were used for the training phase. Results: U-Net architecture can be used to obtain accurate (dice similarity coefficient = 95.72%), fast (21.36 secs), and clinically acceptable and approvable segmentation of the lung region. Conclusions: We have demonstrated that deep learning models can be efficiently applied to rapidly segment and quantify the lung portion of patients having lung diseases, without any supervision of radiologist, in order to produce user-independent results.

KEYWORDS: Deep Learning; lung portion segmentation; U-Net; High Resolution Computed Tomography; radiomics;

I. INTRODUCTION

Biomedical images are a huge source of data which is useful to feed diagnostic tools in order to increase the performance in revealing pathologies. Through radiomics tools, the researchers are able to retrieve informative features from images. The identification of the anatomical region of interest is very crucial to avoid errors in the extraction of the features and their associations with the studied target. Focusing on the region of interest, limits the noise in texture-based feature extraction. Nevertheless, the segmentation process is still a challenging issue in the medical image analysis research area [4,5]. The most common technique used to obtain lung images of patients with lung diseases is high-resolution computed tomography (HRCT). In particular, some challenges have yet to be overcome while segmentation process:

- For HRCT related studies, to get acceptable results analysis of thousands of slices of images is required. Using a supervised segmentation algorithm both visual inspection and manual correction are time-consuming.
- For radiomics analysis, accurate and user-independent segmentations are mandatory for correctly identifying the texture-based prediction model.
- Artificial intelligence approaches are still not being widely applied in clinical practice, mainly due to the requirement of large amounts of labelled training data.

To highlight these issues, we employed a segmentation workflow based on deep learning (DL) using a small dataset of high-resolution CT images. A Deep Learning workflow is defined by following as mentioned: (i) the training/testing data set (ii) outcome variables (iii) training and testing algorithms; and (iv) performance evaluation algorithm. With respect to the machine learning algorithms, Deep Learning requires more data and also it is less transparent, and making it difficult in clinical practice to retrieve from the trained algorithms some medical insights. Several categories of Deep Learning have been developed, including fully convolutional networks, encoder-decoder networks, multi-scale and pyramid network-based models, attention-based models, recurrent neural network-based models and many

more. In our study, we focused on the development of Deep Learning models that provide accurate and fast segmentation results after being trained even with a small image dataset.

Specifically, our dataset consists of 42 high-resolution CT images of patients with lung diseases, out of which only 32 were used for the training process and the remaining 10 were used for the testing process. Out of several Deep Learning algorithms the one that is successfully being applied in the biomedical image segmentation process is the convolutional neural network-based algorithm, U-Net. We compared the efficiency of an enhanced U-NET architecture model and Region growing segmentation for the task of lung portion segmentation from HRCT images. In addition, we implemented the Tversky loss function into the training process, which is applied as it is quite suitable for data augmentation technique, adapted the original Deep Learning models, and we have used the k-fold strategy. In this way, we aimed to enhance the methodology performed by the healthcare operators in the radiomics analyses where an operator-independent segmentation method can be used to extract lung regions and, consequently, to obtain operator-independent results. In the following, to evaluate the performance of U-Net and Region Growing, we considered the accuracy of the segmentation process, amount of training data required, training time and also hardware requirements.

II. RELATED WORK

As our aim was to identify an accurate, and fast and automatic segmentation method of the lung portion without any radiologist supervision, we used the same dataset of images performed in our radiology department. A total of 42 consecutive patients with lung diseases fulfilling these criteria were finally included in the analysis. The patient's ages were ranging from 51 to 82 years. Scans were obtained at a full inspiration from the apex to the lung base with the patients in the supine position. Thin-section CT images were composed of sharp kernel imaging reconstruction and overlapping images. Due to the use of a different CT scanner, the whole dataset had different resolutions as mentioned below:

- 11 studies were obtained using the Philips CT scanner have a matrix resolution of 720×720
- 31 studies were obtained using the GE CT scanner have a matrix resolution of 672×672 .

Deep Learning models typically require all inputs to be of the same size. Consequently, we resampled all datasets to the isotropic voxel size of $1 \times 1 \times 1$ mm³ with a matrix resolution of 256×256 using linear interpolation. From the dataset of 42 patient studies, 32 patient studies were used as both training sets and also as validation sets by using the k-fold strategy (see Section 1.3), while the 10 patient studies (which were not at all used during the training process) were used as a testing set. The grouping was made so that both the sets maintain the same features of the whole dataset (scanner type and patient sex). The ground truth table was obtained by using a semi-automatic and supervised segmentation method, as described in [7], and to discriminate the lungs from other structures (blood vessels and airways) and to eliminate the trachea. Briefly, the digital imaging and communications in medicine (DICOM) images were anonymized using the Osirix software before the automatic HRCT segmentation was obtained using the region growing algorithm.

Voxels that are present within the range of +200 and -1.024 HU were isolated. Successively, the same region growing method was also used to eliminate the trachea. Each scan was then segmented using this conventional image processing method and then manually corrected by an expert thoracic radiologist to create the gold standards. Specifically, the region growing method was able to detect the disease-free lung regions correctly, while some lung regions with high fibrotic areas were not correctly being included in the segmentation process. After the supervised validation process, the segmentation masks were then resampled using the nearest neighbor interpolation and converted into binary values with 0 for background and 1 for the lung region. We used an in-house processing tool which was developed in MATLAB® R2016a running on a windows(3.5 GHz Intel Core i7 processor, 8 GB memory random-access memory; acer Computer) with windows 10 Operating System OS. We implemented the U-Net, and the Tversky loss function using R2019b.

III. METHODOLOGY

1.1 U-Net Architecture

Several changes have been made to the original U-Net architecture to improve segmentation results. All 3×3 convolutions in U-Net were replaced by larger 5×5 convolution operators in order to increase the receptive field of the network. The 5×5 convolutions produced better results in using U-Net for the image segmentation tasks. Each convolution was followed by a drop out layer with a drop-out rate of 10%.

Dropout layers are used to improve regularize the neural network and to avoid overfitting. while the original U-Net architecture does not use padding when applying convolution operators, but we adopted zero padding to ensure that the size of the output feature map has the same size as that of the input size.

The original U-Net architecture had a 2D size of 32 32 and 1024 feature mappings at the down-sampling path's final layer. we used an input size of 256×256 with 32 filters on the first down-sampling path layer, with doubling of the feature maps after each max pool and then stopping at 128 feature maps and a 2D size of 64×64 . Specifically, we refer to i) "feature maps" which are the output of a convolution layer in Deep Learning models highlighting the fact that the input images are converted to the outputs that represent the interesting hidden features present in the input, and to (ii) "max pool" which is the typical operation in convolutional neural networks (CNN) is used to down-sample an input representation. This is typically done by selecting only the maximum value from the non-overlapping rectangular sub-regions of the input.

1.2. Loss Function

Several loss functions have been proposed for calculating the losses occurred during the training process. The dice similarity coefficient (DSC) is majorly used as the loss function in many Deep Learning-based biomedical image segmentation methods, and it measures the overlap between the predicted and the ground truth segmentation masks. Specifically, it is the harmonic mean of false negatives (FNs) and false positives (FPs) and weighs both equally. To adjust the weights of FPs and FNs, the authors in proposed the Tversky index, defined as follows:

$$S(P, G; \alpha \beta) = \frac{|P \cap G|}{|P \cap G| + \alpha|P \setminus G| + \beta|G \setminus P|}$$

where P and G are the set of predicted and ground truth labels, respectively, α and β are the parameters that control the magnitude of penalties of FPs and FNs, respectively, and $P \setminus G$ is the relative complement of G on P. By using the Tversky index, the Tversky loss is defined as shown below:

$$T(\alpha \beta) = \frac{\sum_{i=1}^N p_{0i} g_{0i}}{\sum_{i=1}^N p_{0i} g_{0i} + \alpha \sum_{i=1}^N p_{0i} g_{1i} + \beta \sum_{i=1}^N p_{1i} g_{0i}}$$

where in the output of the final layer of the network (soft-max layer), p_{0i} is the probability of pixel i being the part of lung, and p_{1i} is the probability of pixel that is belonging to the background. In addition, the ground truth training label g_{0i} is set to 1 for lung and it is set to 0 for background, and vice-versa for the label g_{1i} . By adjusting α and β , the trade-off can be controlled between FPs and FNs and setting $\alpha = \beta = 0.5$ leads to the familiar DSC, while setting $\alpha + \beta = 1$ leads to a set of $F\beta$ scores;

1.3. Data Training

In Machine Learning and Deep Learning approaches, the entire dataset is divided into three sets, namely training, validation, testing sets. The testing set is set aside during the training process and it is only used for reporting the final results. In addition, if only a limited amount of data is available for the training process, then in such cases of biomedical image processing, the k-fold cross-validation strategy can be used to achieve efficient training. The whole dataset is divided into k-folds. One of the folds is then treated as validation set and the remaining folds are combined into the training set. This process is repeated several times using each fold as the validation set and the other remaining sets as the training set and hence it is possible to obtain more robust results. Since the considered network model is 2D model, we extracted individual slices from each study in the training fold and these individual slices are used as input to our models.

The performance of the k-fold cross-validation strategy was calculated by averaging the results of all 3 validation folds. Finally, the performance metrics for the U-Net Deep Learning algorithm was calculated on the testing set which was not used at all during the k-fold cross-validation strategy.

Data augmentation is the most common strategy used for training the convolution neural network models, which helps to reduce overfitting, especially in case of limited training data and for each fold, we compute a 2D pixel-wise mean and standard deviation using all training data of that fold. Before being fed into the training pipeline, we have subtracted the mean and then divided by the pre-computed standard deviation.

We used an initial set of 16 patient studies in order to experimentally determine the best learning rates. We used the U-Net model with Adam optimizer and the learning rate is 0.00001 for U-Net model. The Tversky loss function was calculated for every batch size of 8 slices for all experiments, by considering $\alpha = 0.3$ and $\beta = 0.7$. During training process, we allowed each network to train for a maximum of 100 epochs and we used the training loss as the stopping criteria. When the training loss did not decrease for 10 consecutive epochs, we stopped the training.

1.4. Data Analysis

To assess the performance of the automatic segmentation of lung portion, for each clinical case, we computed a set of performance indicators which are routinely used in literature for the comparison. Sensitivity, Specificity, Accuracy, Precision, dice similarity coefficient (DSC), standard variation (std), and confidence interval (CI).

IV. RESULTS

The Performance results for the testing dataset (10 patient studies) were calculated as the average of the results computed from each U-Net trained in the five folds, and using the region growing algorithm. We used the testing Dataset (10 Patients' Studies) to evaluate the results.

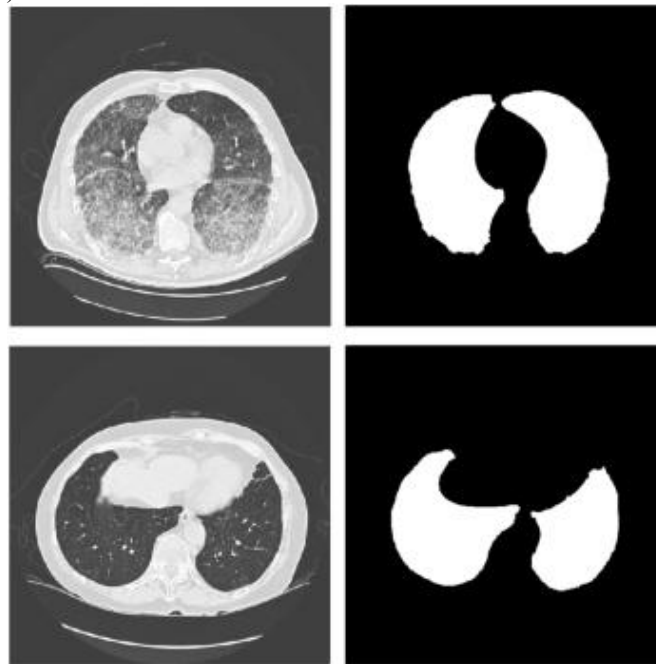


Figure 1. The Lung region segmentation using U-Net Deep Learning Model.

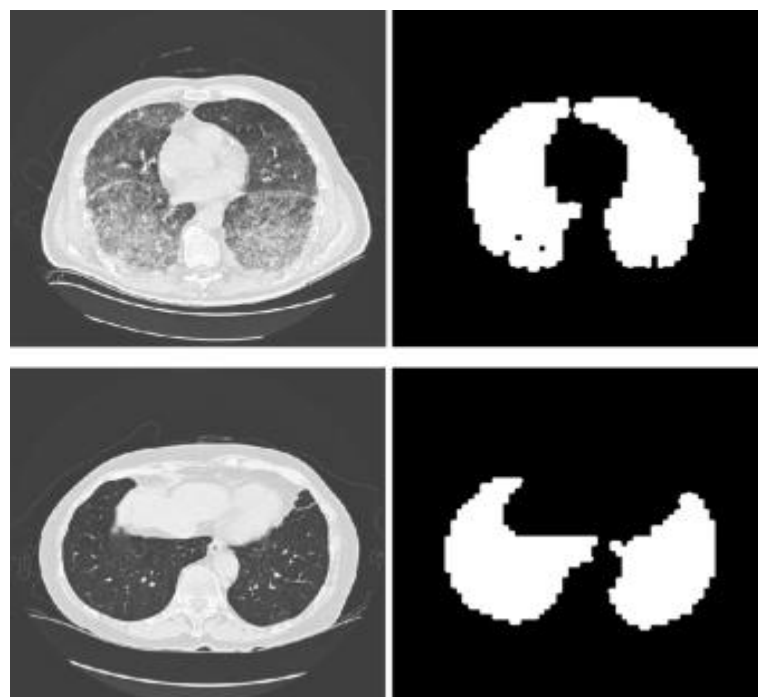


Figure-2: The lung region segmentation by using the Region-Growing technique

Table 1. The Performance results for the validation dataset obtained as the average of the results computed in each loop of the five-fold cross-validation strategy. We used the testing Dataset (10 Patients' Studies) to evaluate the results.

Testing Dataset (consists of 10 Patients' Studies)						
	U-Net			Region Growing		
	Mean	±std	±CI (95%)	Mean	±std	±CI (95%)
sensitivity	96.45%	4.24%	2.66%	97.48%	11.15%	2.37%
Accuracy	98.42%	1.86%	1.16%	85.91%	8.32%	2.23%
specificity	96.34%	3.30%	2.14%	88.15%	11.53%	2.57%
Precision	97.73%	4.42%	2.78%	87.85%	14.40%	3.34%
DSC	95.72%	2.33%	1.97%	89.43%	12.34%	3.52%

To test the differences between the results obtained with the Deep Learning algorithms, we compared the models using an analysis of variance of the DSC computed for all patient's studies. Results calculated are summarized in the Table 1. We have observed that both the methods have achieved a good performance in reducing the difference between the manual and the automated segmentation.

V. CONCLUSION

To extract the lung portion from HRCT images of patients with lung diseases, we demonstrated the feasibility and efficacy of U-Net architecture-based Deep Learning approach using (i) the Tversky loss function into the training process, (ii) the suitable data augmentation technique, and (iii) the cross k-fold strategy. U-Net Deep Learning model highlighted a good segmentation accuracy with a DSC of about 96%, with differences related to the training time and data requirements; results shown by the U-Net were statistically good when compared with the results shown by the region-growing technique. By using our study in the clinical application can not only improve the diagnosis of lung diseases but also the management of the patients through appropriate radiomics studies, where accurate and reproducible segmentations are mandatory, for correctly identifying the prediction model. The future works may also include the implementations with the other deep learning methods (e.g., mentioned in [6]), and to compare them with our results.

REFERENCES

- [1] Sabini, M.G.; Russo, G.; Ippolito, M. Using an automated segmentation method in initial radiomics observation of brain metastases. *BMC Bioinform.* 2020, 21, 325. [CrossRef] [PubMed]
- [2] Verde, F.; Creta, M.; Pace, L.; Cuocolo, R.; Stanzone, M.; Imbriaco, M. Detection of prostate cancers with the use of MRI: A radiomic form capabilities observe. *Eur. J. Radiol.* 2019, 116, 144–149. [CrossRef] [PubMed]
- [3] Comelli, A.; Stefano, A.; Coronello, C.; Russo, G.; Vernuccio, F.; Cannella, R.; Salvaggio, G.; Lagalla, R.; Barone, S. Radiomics: A New Biomedical Workflow for Creating a Predictive Model. In *Annual Conference on Medical Image Understanding and Analysis*; Springer: Berlin/Heidelberg, Germany, 2020; pp. 280–293.
- [4] Comelli, A.; Bignardi, S.; Stefano, A.; Russo, G.; Sabini, M.G.; Ippolito, M.; Yezzi, A. Developing a brand new absolutely third-dimensional technique for tumours delineation within the physiological images. *Comput. Biol. Med.* 2020, 120, 103701. [CrossRef] [PubMed]
- [5] Comelli, A. PET Image Segmentation by using a Fully three-Dimensional Active Surface with Machine Learning. *J. Imaging* 2020, 6, 113. [CrossRef]
- [6] Christe, A.; Peters, A.A.; Drakopoulos, D.; Heverhagen, J.T.; Geiser, T.; Stathopoulou, T.; Christodoulidis, S.; Anthimopoulos, M.; Mouggiakakou, S.G.; Ebner, L. Computer-Aided Diagnosis of Pulmonary Fibrosis Using Deep Learning and CT Images. *Invest. Radiol.* 2019, 54, 627–632. [CrossRef]
- [7] Stefano, A.; Gioè, M.; Russo, G.; Palmucci, S.; Basile, A.; Comelli, A.; Benfante, V.; Sambataro, G.; et al. Performance of the Features of Radiomics within the Quantification of lung diseases from HRCT. *Diagnostics* 2020, 10, 306. [CrossRef]
- [8] Grassedonio E.; Russo G. et al. Assessment of Lung Cancer Development in Patients having lung diseases Using Quantitative High-Resolution Computed Tomography: A Retrospective Analysis. *J. Thorac. Imaging* 2019, 35, 115–122. [CrossRef]



- [9] Torrisi, S.E.; Palmucci, S.; Stefano, A.; Russo, G.; Torcitto, A.G.; Falsaperla, D.; Gioè, M.; Pavone, M.; Vancheri, A.; Sambataro, G.; et al. Assessing the survival of the patients with idiopathic pulmonary fibrosis with the use of quantitative High Resolution CT indexes. *Multidiscip. Respir. Med.* 2018, 13, 1–8.[CrossRef]
- [10] Laudicella, R.; Comelli, A.; Crocè, L.; Vento, A.; Spataro, A.; Comis, A.D.; La Torre, F.; Gaeta, M.; et al. Convolutional Neural Networks in Cardiovascular Diseases and its Potential in Clinical Application in Molecular Imaging. *Curr. Radiopharm.* 2020.[CrossRef]



INNO  **SPACE**
SJIF Scientific Journal Impact Factor
Impact Factor: 7.542



ISSN INTERNATIONAL
STANDARD
SERIAL
NUMBER
INDIA



INTERNATIONAL JOURNAL OF INNOVATIVE RESEARCH

IN COMPUTER & COMMUNICATION ENGINEERING

 **9940 572 462**  **6381 907 438**  **ijircce@gmail.com**



www.ijircce.com

Scan to save the contact details